

# Influence of microstructure on phase transformation behavior and mechanical properties of plasma arc deposited shape memory alloy

Bingwen Lu<sup>a,b</sup>, Xiufang Cui<sup>a,\*</sup>, Erbao Liu<sup>a</sup>, Xiangru Feng<sup>a</sup>, Meiling Dong<sup>a</sup>, Yang Li<sup>a</sup>, Haidou Wang<sup>b</sup>, Guo Jin<sup>a,\*</sup>

<sup>a</sup> Institute of Surface/Interface Science and Technology, Key Laboratory of Superlight Material and Surface Technology of Ministry of Education, College of Material Science and Chemical Engineering, Harbin Engineering University, Harbin 150001, China

<sup>b</sup> National Key Laboratory for Remanufacturing, Armored Forces Engineering Institute, Beijing 100072, China

## ARTICLE INFO

### Keywords:

Additive manufacturing, plasma arc deposition  
TiNi alloy  
Ti<sub>2</sub>Ni phase  
Phase transformation  
Quasi-linear superelasticity

## ABSTRACT

Recently, additive manufacturing have gradually become an attractive processing technology for TiNi alloy. In this work, the Ti<sub>50</sub>Ni<sub>50</sub> alloy was successfully prepared by plasma arc deposition (PAD) technology. The microstructures, phase transformation characteristics and mechanical properties were investigated in detail. The PAD-TiNi alloy mainly comprised of TiNi (B2), TiNi (B19') and Ti<sub>2</sub>Ni phases. The TiNi cellular crystals, TiNi dendrite crystals and TiNi equiaxed crystals were presented at the bottom, middle and top area of PAD-TiNi alloys, respectively. Some irregular Ti<sub>2</sub>Ni phases were distributed in the inter-dendritic areas. The peritectic reaction of  $L(\text{Ti}) + \text{TiNi} \rightarrow \text{Ti}_2\text{Ni}$  led to the formation of irregular Ti<sub>2</sub>Ni phases. The coherence of Ti<sub>2</sub>Ni phases and TiNi matrix phases drove the two-step phase transformation (B2 → R → B19') during the cooling process. The as-deposited samples showed favorable hardness and high strength, especially possessing special quasi-linear superelasticity (up to 3.8%) with narrow hysteresis, which was derived from the quick appearance and disappearance of deformation microtwins under loading and unloading condition. The newly formed interface between Ti<sub>2</sub>Ni precipitates and TiNi matrix phase offered the nucleation sites for deformation microtwins and promoted the formation of microtwins.

## 1. Introduction

TiNi alloy is an attractive material for engineering applications owing to its unique shape memory effect, superelasticity effect, high damping properties, fatigue resistance, and other properties [1,2]. Up to now, several conventional processing technologies (including induction melting, casting, sintering and powder metallurgy) have been successfully employed to manufacture small-scale and simple TiNi alloy components (rod, sheet, wires, etc.). However, it is still difficult to fabricate large-scale and complex-shaped TiNi alloy components due to high reactivity and high ductility of TiNi alloy [3–5]. Recently, additive manufacturing (AM) technology has drawn significant attention to the direct formation of complex TiNi alloy parts due to its unique advantages, such as shape complexities, material complexities and functional complexities [6].

This AM technology of fabricating TiNi alloy components is also known as 4D printing [7]. The 4D printing is exactly the combination of AM technology and smart materials. As a classical shape memory material, TiNi alloy shows a great potential in 4D printing, and some

related studies on laser additive manufacturing (selective laser melting, laser engineered net shaping, laser direct deposition, etc.) of TiNi alloy have been carried out in recent years [6,8–12]. Plasma arc deposition (PAD) is also an AM technology with a plasma arc as the heat source. PAD has some considerable advantages over conventional AM techniques in higher deposition rate, great convenience, lower consumption and safety reliability, which demonstrates its enormous potential to fabricate large-scale components [13,14]. PAD has been reported in many studies to produce parts of stainless steel, titanium alloys and aluminum alloys [15]. Hence, PAD will be another significant AM techniques to fabricate large-scale TiNi alloy components. Therefore it is reasonable to believe that this technology will broaden the application of TiNi alloys. However, there are few research reports focusing on the PAD manufactured TiNi alloys. In order to promote its engineering application, it is needed to systematically research on the phase transformation characteristic and thermomechanical response of PAD manufactured TiNi alloy.

In this paper, PAD technique was adopted to synthesize TiNi alloy. The formation mechanism of microstructure was investigated, and the

\* Corresponding authors.

E-mail addresses: [cuixf721@163.com](mailto:cuixf721@163.com) (X. Cui), [jinjg721@163.com](mailto:jinjg721@163.com) (G. Jin).

<https://doi.org/10.1016/j.msea.2018.08.098>

Received 5 June 2018; Received in revised form 9 August 2018; Accepted 27 August 2018

Available online 30 August 2018

0921-5093/© 2018 Elsevier B.V. All rights reserved.

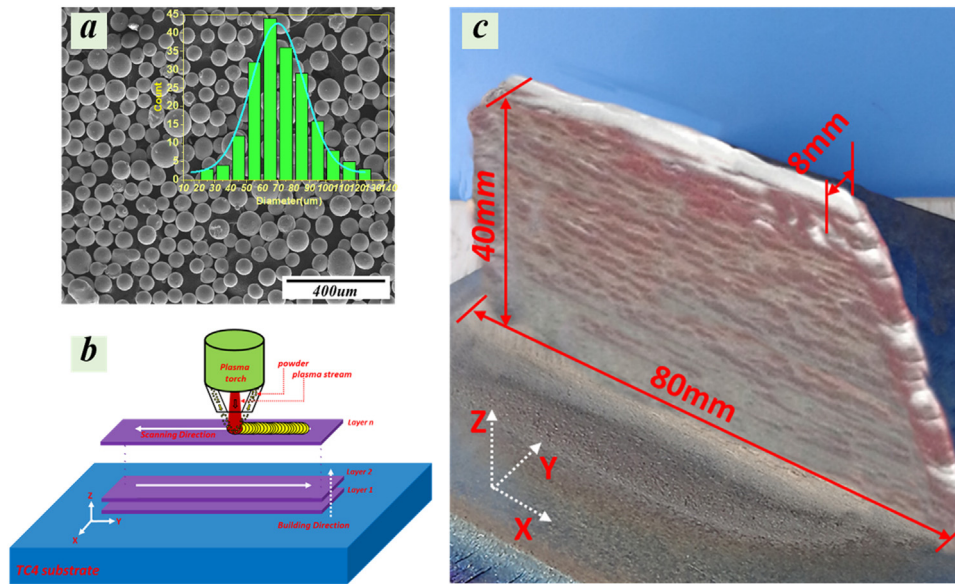


Fig. 1. (a) SEM image of powder and particle distribution, (b) schematic of additive manufacturing path and (c) specimen of PAD-TiNi alloy.

relationship between microstructure and phase transformation characteristic, thermomechanical response was also studied systematically.

## 2. Materials and methods

$\text{Ni}_{50}\text{Ti}_{50}$  (at%) pre-alloyed spherical powders were used as the raw materials with purity higher than 99.9%. The size range of the powder particle was confirmed to be about 25–125  $\mu\text{m}$  by scanning electron microscopy (SEM) micrographs (Fig. 1a) with the help of *ImageJ* software. Ti6Al4V (TC4) was selected as the substrate, which was first cut to a sheet with the dimensions of 200 mm (length)  $\times$  100 mm (width)  $\times$  8 mm (height), then polished and cleaned thoroughly with acetone. Samples were fabricated via a plasma arc deposition system (including plasma arc deposition source, protection device, depositing torch and computer control unit). The whole manufacture process was in an Ar atmosphere with the oxygen-content  $< 50$  ppm. The powders were deposited layer by layer onto the substrate to form rectangle specimens with the dimensions (x, y, z) of  $80 \times 40 \times 8 \text{ mm}^3$  (Fig. 1c). The schematic of additive manufacturing path was shown in Fig. 1b. The scan direction of each path was opposite to that of the previous one until a layer was completed deposited. Then laser head raised the same height for every layer and the above process was repeated until the entire object represented was fabricated on the substrate. The manufacturing parameters of PAD were presented in Table 1.

The phase structure of all samples was analyzed by a BRUKER-D8 X-ray diffraction (XRD) with Cu target,  $K_{\alpha}$  radiation, tube voltage of 40 kV, tube current of 40 mA and scanning speed of  $5^{\circ}/\text{min}$ . Microstructure was investigated by an optical microscope (OM, Carl Zeiss, Germany) and a scanning electron microscope (SEM, FEI Quanta 200, Netherlands) with an acceleration voltage of 20 kV, equipped with an energy dispersive spectrometer (EDS). The samples for metallographic test were mechanically polished and etched for 10–30 s using

Table 1  
Manufacturing parameters of PAD.

Work current (A)	150
Scanning speed (mm/s)	3
Powder feeding (g/min)	3.5
Plasma gas flow (L/min)	0.3
Shield gas flow (L/min)	15
Overlapping ratio (%)	40
Z-axis increment (mm)	2.3

$\text{H}_2\text{O}$  (80%) +  $\text{HNO}_3$  (15%) +  $\text{HF}$  (5%). The transformation temperatures (TTs) was detected by a DSC204F1 differential scanning calorimetry (DSC, NETZSCH, German) with a heating and cooling rate of  $10^{\circ}\text{C}/\text{min}$  from  $-80$ – $100^{\circ}\text{C}$ . The micro-hardness was measured by a HVS-1000 micro hardness tester with a load of 200 g and a loading time of 15 s. Compression test was performed by the 100 kN INSTRON4505 electronic universal testing machine (INSTRON, America) using cylinder samples with the size of 4 mm in diameter and 8 mm in length. To analyze super-elastic behavior, all samples were heated to temperatures above the  $A_f + 15^{\circ}\text{C}$  and held for 10 min, then loaded up at a strain rate of  $0.001 \text{ s}^{-1}$  and unloaded with the rate of 100 N/s.

## 3. Results

### 3.1. Microstructure

Fig. 2 displays the XRD patterns of PAD TiNi alloy at room temperature. The feedstock powder only consists of TiNi (B2) austenite phase. However, phase analysis reveals the existence of TiNi (B2) (PDF 65–5537), TiNi (B19') (PDF 35–1281) and  $\text{Ti}_2\text{Ni}$  (PDF 72–0442) of as-deposited samples. Compared with the feedstock powder, the peak

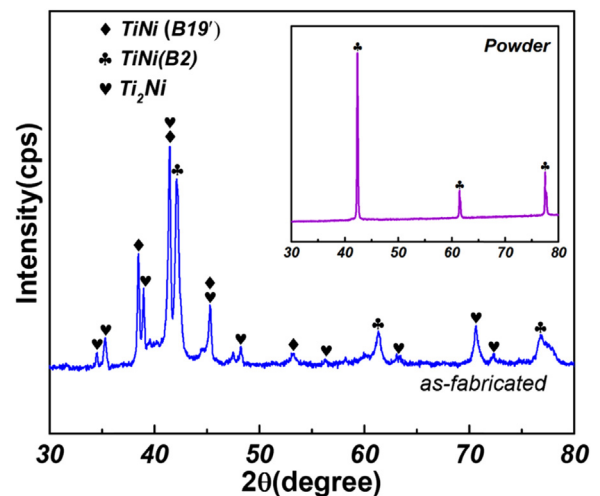


Fig. 2. XRD spectra of PAD-TiNi alloy at different states.

Download English Version:

<https://daneshyari.com/en/article/10142003>

Download Persian Version:

<https://daneshyari.com/article/10142003>

[Daneshyari.com](https://daneshyari.com)